

# Journal of MARINE RESEARCH

---

Volume 46, Number 3

## The coupling of wave drift and wind velocity profiles

by John A. T. Bye<sup>1</sup>

### ABSTRACT

The Stokes drift velocity profile due to Toba's equilibrium wave spectrum is shown to consist of a surface constant shear layer, an intermediate logarithmic layer and a deep exponentially decaying tail. On identifying the logarithmic layer with a wall boundary layer (which is justified *a posteriori* by showing that the major part of the energy dissipation by wave breaking occurs in the roughness sublayer), for a range of directionality ( $p$ ) of the wave spectrum  $1/2-2$ , Toba's constant ( $\alpha$ ) lies in the range 0.12–0.10 in good agreement with data. The roughness length for water ( $z_0$ ) of this profile has the Charnock form,  $z_0 = au_*^2 g^{-1}$  in which  $u_*$  is the friction velocity in air,  $g$  is the acceleration of gravity and  $a$  is a constant of order unity determined by the condition that momentum transfer by wave breaking just supports the wind stress, and using this formula the transition from smooth to intermediate flow at which rippling commences is quite well estimated. The velocity profiles in air and water with respect to  $z_0$ , are predicted from a similarity hypothesis to have the forms,

$$u' = u_* \left( \gamma + \frac{1}{\kappa} \ln \frac{z}{z_0} \right)$$
$$u = w_* \left( \gamma - \frac{1}{\kappa} \ln \frac{z}{z_0} \right) \quad z > z_0$$

where  $z$  is the distance from the sea surface,  $u'$  and  $u$  are respectively the velocities in air and water,  $\kappa$  is Von Karman's constant,  $w_*$  is the friction velocity in water,  $\gamma w_*$  is the Stokes surface drift velocity, and  $\gamma u_*$  is a wave speed centered in the equilibrium range. Observations in the open sea indicate that  $\gamma \sim 12$ .

1. The Flinders Institute for Atmospheric and Marine Sciences, The Flinders University of South Australia, Bedford Park, S.A., 5042.

An alternate pair of profiles, also predicted from the similarity hypothesis, is,

$$u' = u_s + \frac{u_*}{\kappa} \ln \frac{z}{z'_0}$$

$$u = u_s - \frac{w_*}{\kappa} \ln \frac{z}{z'_0} \quad z > z'_0$$

where  $z'_0$  is the roughness length for air, and  $u_s \sim 2\gamma w_*$  is the surface current. Observations suggest that small surface drifters travel at speeds intermediate between  $\gamma w_*$  and  $2\gamma w_*$ .

## 1. Introduction

The air-sea interface is of great importance in the large scale dynamics of the atmosphere and ocean. A fundamental problem is the relation between waves and turbulence. We consider this problem for a wave field in which the major part of the wave energy is contained in an equilibrium range of the form originally proposed by Toba (1973). A particular aim is to calculate the Stokes drift velocity profile for this equilibrium range (Section 3), and to relate this drift profile to the velocity profile in air, which in turn is a function of the wave speed of the gravity waves centered in the equilibrium range. This is done using a similarity hypothesis for the coupled boundary layer (Section 5).

The analysis has been stimulated by some recent observations in the San Diego Model Yacht Pond (Bye, 1987) in which simultaneous measurements were made in air and water.

## 2. The wavenumber spectrum in the equilibrium range

In the equilibrium range, there are strong arguments (Phillips, 1985) in support of an energy input at all wavenumbers ( $\mathbf{k}$ ) by wind and of energy dissipation at all wavenumbers by wave breaking, and also of a negative spectral divergence between these two processes which requires a net energy flux into the equilibrium range from the low wavenumbers. This energy balance for growing wind waves is illustrated by the composite data set of Toba *et al.* (1985) which has the following properties:

(a) The amplitude of the significant waves is represented by the 3/2 power "law,"

$$a_s = \frac{1}{2} B u_*^{1/2} g^{1/2} \left( \frac{2\pi}{\sigma_s} \right)^{3/2} \quad (1)$$

in which  $a_s$  and  $\sigma_s$  are respectively the wave amplitude and angular frequency of the significant wave,  $g$  is the acceleration of gravity,  $u_* = (\tau_s/\rho')^{1/2}$  is the friction velocity in air in which  $\tau_s$  is the surface shearing stress,  $\rho'$  is the density of air, and  $B$  is a constant.

From Eq. (1), we obtain the wave slope,

$$a_s k_s = \frac{1}{2} (2\pi)^{3/2} B \left( \frac{u_*}{c_s} \right)^{1/2}$$

in which  $k_s$  is the wavenumber, and  $c_s = (g/k_s)^{1/2}$  is the Stokes wave speed of the significant wave. This quantity increases with  $k_s^{1/4}$  indicating a gradual increase in the degree of saturation with wavenumber throughout the equilibrium range.

(b) The total wave energy is of the form,

$$E = \bar{\zeta}^2 = B_s u_* g \sigma_0^{-3}$$

where  $\bar{\zeta}^2$  is the mean square surface displacement,  $\sigma_0 = 0.95 \sigma_s$  is the peak frequency of the wave spectra, and  $B_s$  is a constant.

(c) The equilibrium range in the two-dimensional wavenumber spectrum (Phillips, 1985) is,

$$\psi(\mathbf{k}) = \beta (\cos \theta)^p u_* g^{-1/2} k^{-7/2} \quad (2)$$

in which

$$\bar{\zeta}^2 = \int_0^\infty \int_{-\pi/2}^{\pi/2} \psi(\mathbf{k}) k \, d\theta \, dk$$

where  $\mathbf{k} = (k, \theta)$ ,  $\beta$  is a constant,  $\theta$  is the angle of propagation of the wave ( $\mathbf{k}$ ) to the wind direction,  $\zeta$  is the surface elevation and  $p$  is a constant which specifies the directionality of the wave spectrum.

The frequency spectrum which corresponds with Eq. (2) is,

$$\begin{aligned} \phi(\sigma) &= 2 \int_{-1/2\pi}^{1/2\pi} k \Psi(\mathbf{k}) \left( \frac{\partial \sigma}{\partial k} \right)^{-1} d\theta \Big|_{k=\sigma^2/g} \\ &= \alpha u_* g \sigma^{-4} \end{aligned} \quad (3)$$

where  $\bar{\zeta}^2 = \int_0^\infty \phi(\sigma) \, d\sigma$  in which  $\alpha = 4\beta I(p)$  is Toba's constant (Phillips, 1985), and

$$I(p) = \int_{-1/2\pi}^{1/2\pi} (\cos \theta)^p \, d\theta = B \left( \frac{1}{2}, \frac{1}{2} (p + 1) \right) \quad (4)$$

where  $B(m, n)$  is the beta function.

The composite data set of Toba *et al.* (1985) yields the following values for the constants,  $B = 0.062$  and  $B_s = 0.051$  and for Toba's constant,  $\alpha = 0.096$ .

In the determination of the drift velocity profile, we will use as a model for the total wave spectrum, an equilibrium range (Eq. (3)) bounded by a lower limit ( $\sigma_0$ ) and an upper limit ( $\sigma_1$ ) where  $\sigma_1 \gg \sigma_0$ . For this model, on integrating Eq. (3), the total energy,

$$E = \frac{1}{3}\alpha u_* g \sigma_0^{-3} \quad \sigma_1 \gg \sigma_0. \tag{5}$$

Using  $\alpha = 0.096$ , this model spectrum (Eq. (5)) predicts  $B_\sigma = 0.032$ , the discrepancy between this value and the observed value ( $B_\sigma = 0.051$ ) being due to the use of a lower frequency limit in the model spectrum in place of the low frequency tail of the observed spectra. A consideration of the tail is beyond the scope of our analysis which focusses on the velocity profiles in the coupled boundary layer.

**3. The wave drift profile**

We construct the drift profile and transport by integrating the Stokes velocity (Stokes, 1847) and transport for each component of the spectrum respectively,

$$u(k) = a^2 g^{1/2} k^{3/2} e^{-2kz} \tag{6}$$

and

$$T(k) = \frac{1}{2} a^2 g^{1/2} k^{1/2} \tag{7}$$

where  $a$  is the amplitude of the wave ( $\mathbf{k}$ ), and  $z$  is depth,  $z = 0$  being the undisturbed sea surface.

Then since,

$$\frac{1}{2} a^2 = \psi(\mathbf{k}) d\mathbf{k}$$

using Eqs. (3) and (4) and integrating over the spectrum, we obtain,

$$u = 4\beta I(p + 1) u_* \int_{k_0}^{k_1} k^{-1} e^{-2kz} dk \tag{8}$$

and

$$T = 2\beta I(p + 1) u_* [k_0^{-1} - k_1^{-1}] \tag{9}$$

where  $k_0 = \sigma_0^2/g$  and  $k_1 = \sigma_1^2/g$ .  $u$  and  $T$  are respectively the drift velocity of a water particle at  $z$ , and the volume transport/unit width of the drift current. This procedure follows that adopted in Bye (1967), Chang (1969) and Kenyon (1969).

On expressing these results in terms of Toba's constant using Eq. (3), and defining a nondimensional length,  $Z = zg/u_*^2$  and a nondimensional wavenumber,  $K = u_*^2 k/g$  we have the alternate forms,

$$u = \alpha' u_* \int_{K_0}^{K_1} K^{-1} e^{-2KZ} dK \tag{10}$$

and

$$T = \frac{1}{2} \alpha' u_*^3 g^{-1} [K_0^{-1} - K_1^{-1}] \tag{11}$$

where

$$\alpha' = \alpha \frac{I(p+1)}{I(p)}$$

and the expression for the velocity shear,

$$\frac{du}{dZ} = -\frac{\alpha' u_*}{Z} [e^{-2K_1 Z} - e^{-2K_0 Z}]. \quad (12)$$

For an intermediate range of depth Eq. (12) reduces to the approximate expression,

$$\frac{du}{dZ} = -\frac{\alpha' u_*}{Z}; \quad (2K_1)^{-1} \ll Z \ll (2K_0)^{-1} \quad (13)$$

over which range we find that,

$$u = -\alpha' u_* \ln Z + \text{const.} \quad (14)$$

These results are independent of either the high or low limit wavenumbers.

In the surface layer on the other hand, the velocity shear tends to the constant value,

$$\frac{du}{dZ} = -2K_1 \alpha' u_*, \quad Z \ll (2K_1)^{-1} \quad (15)$$

which depends on the high wavenumber limit only, and at great depths ( $Z \gg (2K_0)^{-1}$ ) the shear tends to zero exponentially.

The complete velocity profile found from Eq. (10) by quadrature shows the intermediate logarithmic profile, and "tails" of reduced slope at smaller and greater depths (cf. Fig. 1).

For  $Z \rightarrow 0$ , Eq. (10) may be integrated directly to give the reference current,

$$u_0 = \alpha' u_* \ln \frac{K_1}{K_0} \quad Z \ll (2K_1)^{-1} \quad (16)$$

$u_0$  is the surface drift current due to the Stokes wave spectrum only. Its relation to the (true) surface current ( $u_s$ ) is discussed in Section 5. Note that on a semi-logarithmic graph the surface layer of constant shear appears to the eye as a layer of constant velocity.

Eq. (13) predicts a logarithmic profile over an extended range of depth as a consequence of the equilibrium spectrum. This is in accord with many data sets (Csanady, 1984). Furthermore on expressing Eq. (13) in terms of the friction velocity in water,  $w_* = (\tau_s/\rho)^{1/2}$  in which  $\rho$  is the density of water, and assuming that the logarithmic velocity profile is a wall boundary layer, we have the relation,

$$\alpha' = \left(\frac{\rho'}{\rho}\right)^{1/2} \kappa^{-1} \quad (17)$$

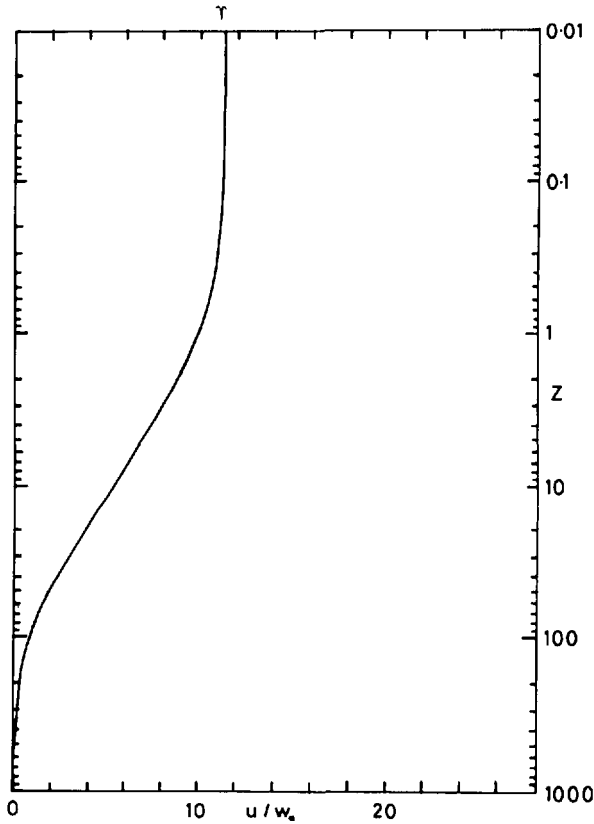


Figure 1. Drift velocity profiles due to Toba's equilibrium spectrum. With nondimensional wavenumber limits  $K_1 = 0.35$ ,  $K_0 = 0.0035$ , and  $\alpha' = 0.085$ .

where  $\kappa$  is Von Karman's constant. On now assuming that  $\kappa = 0.4$ ,  $\rho = 1000 \text{ kg m}^{-3}$  and  $\rho' = 1.2 \text{ kg m}^{-3}$ , Eq. (17) predicts that,

$$\alpha' = 0.09 \quad (18)$$

and hence that Toba's constant,

$$\alpha = 0.09I(p)/I(p+1). \quad (19)$$

Since  $I(0)/I(1) = \pi/2$  and  $I(p)/I(p+1) \rightarrow 1$  as  $p \rightarrow \infty$ , this interesting relationship indicates that Toba's constant lies in the range,

$$0.14 > \alpha > 0.09$$

which accords with the composite data set of Toba *et al.* (1985) and with other observations in the open sea (Phillips, 1985). Its value *decreases* as the directionality ( $p$ ) of the wave spectrum *increases*. Observations of  $p$  (Phillips, 1985) lie in the interval  $1/2-2$ , for which  $\alpha$  would have the somewhat narrower range of 0.12-0.10.

The identification of the wall boundary layer with the wave boundary layer is justified in Section 6 after a similarity hypothesis for the coupled boundary layer has been introduced.

#### 4. The Charnock relation for water

On substituting Eq. (17) in Eq. (15) we obtain the explicit expression for the surface shear,

$$\frac{du}{dz} = - \frac{2K_1 g \rho'}{\kappa w_* \rho} \quad (20)$$

and on assuming that the shearing stress is constant, the kinematic eddy viscosity,

$$A_0 = \frac{\kappa w_*^3 \rho}{2K_1 g \rho'} \quad (21)$$

and the aerodynamical roughness length for water,

$$z_0 = \frac{A_0}{\kappa w_*} = \frac{1}{2K_1} \frac{u_*^2}{g} \quad (22)$$

Phillips (1985) estimates that  $K_1$  lies in the range  $0.2 \lesssim K_1 \lesssim 0.5$ . The argument is that the high wavenumber limit is determined essentially by the condition that the momentum transfer by wave breaking in the equilibrium range between the limits  $K_1$  and  $K_0$ , is just sufficient to support the wind stress.

Thus for the mean value  $K_1 = 0.35$ , on substituting in Eq. (22) we have,

$$z_0 = a u_*^2 g^{-1} \quad (23)$$

where

$$a = \frac{1}{2K_1} \sim 1.4.$$

Eq. (23) restores dimensional dignity to the Charnock (1955) relation as referred to *water*. In a moderate breeze ( $u_* = 0.3 \text{ m s}^{-1}$ ),  $z_0 \sim 1 \text{ cm}$ .

Furthermore, the transition to rough flow (in water) occurs at the friction velocity ( $w_*^R$ ) given by the relation,

$$\frac{w_*^R z_0}{\nu} = \kappa^{-1}$$

where  $\nu$  is the kinematic viscosity of water which yields,

$$u_*^R = \left( \frac{g\nu}{\kappa a} \right)^{1/3} \left( \frac{\rho'}{\rho} \right)^{-1/6} \quad (24)$$

and the transition to smooth flow occurs at,

$$u_*^S = \left( \frac{b' g \nu}{a} \right)^{1/3} \left( \frac{\rho'}{\rho} \right)^{-1/6}$$

where  $b' = 0.11$  (Schlichting, 1960).

On assuming that  $\nu = 1.3 \cdot 10^{-6} \text{ m}^2 \text{ s}^{-1}$  and  $a = 1.4$  we find that  $u_*^R = 0.086 \text{ m s}^{-1}$ , ( $w_*^R = 0.29 \text{ cm s}^{-1}$ ) and  $u_*^S = 0.030 \text{ m s}^{-1}$  ( $w_*^S = 0.10 \text{ cm s}^{-1}$ ). The minimum wavelength ( $\lambda_1$ ) in the model wave spectrum is related to  $z_0$  by the expression,

$$\lambda_1 = 4\pi z_0$$

and on evaluating  $\lambda_1$  at the transitional friction velocities, we obtain,

$$\lambda_1^R = 4\pi \left( \frac{\rho}{\rho'} \frac{a \nu^2}{g \kappa^2} \right)^{1/3} \quad (25)$$

and

$$\lambda_1^S = 4\pi \left( \frac{\rho}{\rho'} \frac{a \nu^2 b'^2}{g} \right)^{1/3}$$

from which  $\lambda_1^R = 14 \text{ mm}$  and  $\lambda_1^S = 2 \text{ mm}$ .

These predictions appear to be of the correct order of magnitude to describe the conditions under which gravity waves are initiated on a water surface, although the criteria for onset are not well defined. On comparing our estimates with the laboratory studies of wave generation of Kahma and Donelan (1987) we note that,

- (a) the transition to smooth flow occurs at a frictional velocity similar to that of  $0.02 \text{ m s}^{-1}$  at which positive growth rates are first observed, and  $\lambda_1^S < \lambda^C$  where  $\lambda^C = 17 \text{ mm}$  is the critical wavelength above which gravity dominates surface tension as the force governing the wave motion, and at which the wave speed is a minimum.
- (b) in the intermediate range ( $u_*^S - u_*^R$ ) observed growth rates are much greater than predictions from the viscous shear flow instability mechanism.
- (c) the transition to rough flow occurs about at the friction velocity ( $\sim 0.10 \text{ m s}^{-1}$ ) where the growth rates increase sharply and also are predicted quite well by the instability mechanism, and the wavelength ( $\lambda_1^R$ ) is similar to the critical wavelength ( $\lambda^C$ ).

Thus the range of friction velocities ( $u_*^S - u_*^R$ ) corresponds with the range of growth in which Kahma and Donelan (1987) deduce that both the instability and the resonance mechanisms of wave generations may contribute, and the range ( $> u_*^R$ ) corresponds to the region in which the instability mechanism is dominant. These results suggest that

the Charnock relation (Eq. (23)) adequately describes conditions over the complete range of wind speeds for which gravity waves are generated.

We also have from Eq. (21) that the eddy viscosity in the surface layer,

$$A_0 \sim 50 w_*^3 \text{ m}^2 \text{ s}^{-1} \quad (26)$$

and (by definition) from Eq. (22) that,

$$R = \frac{w_* z_0}{A_0} = \kappa^{-1}, \quad (27)$$

Churchill and Csanady (1983) determined these quantities from water velocity profiles by estimating the velocity shear in the top 5 cm for  $w_* \sim 0.01 \text{ m s}^{-1}$ . The results ( $A_0 \sim 10^{-4} \text{ m}^2 \text{ s}^{-1}$ ,  $R \sim 0.7$ ) are in fair agreement with Eqs. (26) and (27). The discrepancies may have been due to fitting the linear velocity profile over somewhat too great a depth for the constant shear limit to be a good approximation. Eq. (15) indicates that the depth of the constant shear layer during the observations would have been about 1 cm.

### 5. A similarity hypothesis for the coupled air-sea boundary layer

In the intermediate range of depth, we have the approximate logarithmic profile,

$$u = u_0 - \frac{w_*}{\kappa} \ln \frac{z}{z_0} \quad (28)$$

in which from Eq. (16) using Eq. (17), the reference current (speed),

$$u_0 = \frac{w_*}{\kappa} \ln \frac{K_1}{K_0}. \quad (29)$$

Eq. (28) has the properties that  $u = u_0$  at  $z = z_0$ , and  $u = 0$  at  $z = z_1$  where

$$z_1 = \frac{1}{2K_0} \frac{u_*^2}{g}.$$

The corresponding logarithmic layer in air is

$$u' = u_s + \frac{u_*}{\kappa} \ln \frac{z}{z'_0} \quad (30)$$

in which  $u'$  is the air velocity at height  $z$ ,  $u_s$  is the surface current, and  $z'_0$  is the roughness length for air.

An empirical relation for  $z'_0$  is

$$z'_0 = a' \frac{u_*^2}{g} \quad (31)$$

in which the average of several sets of observations in the open sea, summarized by Wu (1982), indicates that  $a' = 0.0185$ , and observations of long-fetch data (Smith, 1980) are consistent with a lower value,  $a' \sim 0.01$ .

Eqs. (28) and (30) may be written in a similarity form by transformations of the reference velocity such that, either,

$$\begin{aligned} u &= u_0 - \frac{w_*}{\kappa} \ln \frac{z}{z_0} & z > z_0 \\ u' &= u'_0 + \frac{u_*}{\kappa} \ln \frac{z}{z_0} \end{aligned} \quad (32)$$

where

$$u'_0 = u_s + \frac{u_*}{\kappa} \ln \frac{z_0}{z'_0} \quad (33)$$

in which  $u'_0$  is the reference wind (speed) at  $z = z_0$ , or

$$\begin{aligned} u &= u'_s - \frac{w_*}{\kappa} \ln \frac{z}{z'_0} & z > z'_0 \\ u &= u_s + \frac{u_*}{\kappa} \ln \frac{z}{z'_0} \end{aligned} \quad (34)$$

where

$$u'_s = u_0 + \frac{w_*}{\kappa} \ln \frac{z_0}{z'_0}. \quad (35)$$

On noting that  $z'_0 < z_0$  and applying the similarity hypothesis, we require the auxiliary relations,

$$u_0 = \gamma w_*, u'_0 = \gamma u_* \quad (36)$$

where  $\gamma$  is a constant, and

$$u'_s = u_s \quad (37)$$

such that the velocity is continuous across the interface at  $z'_0$ . These conditions together with the defining relation,  $w_* = (\rho'/\rho)^{1/2} u_*$  allow explicit expressions to be obtained for  $\gamma$  and  $u_s$ , namely,

$$\gamma = \frac{1}{\kappa} \ln \left( \frac{a}{a'} \right)^{(1+\epsilon)/(1-\epsilon)} \quad (38)$$

and

$$u_s = \frac{2\gamma}{1 + \epsilon} w_* \tag{39}$$

where  $\epsilon = (\rho'/\rho)^{1/2}$ , together with the two pairs of similarity profiles,

$$\begin{aligned} u &= w_* \left( \gamma - \frac{1}{\kappa} \ln \frac{z}{z_0} \right) \\ u' &= u_* \left( \gamma + \frac{1}{\kappa} \ln \frac{z}{z_0} \right) \quad z > z_0 \end{aligned} \tag{40}$$

and

$$\begin{aligned} u &= u_s - \frac{w_*}{\kappa} \ln \frac{z}{z'_0} \\ u' &= u_s + \frac{u_*}{\kappa} \ln \frac{z}{z'_0} \quad z > z'_0 \end{aligned} \tag{41}$$

which are illustrated in Figure 2. The profile pair (Eq. (41)) predicts cf. Bye (1985), that

$$u_s = \frac{\mathbf{u} + \epsilon \mathbf{u}'}{1 + \epsilon} \tag{42}$$

and the ratio of the dissipation rates in the two fluids in the layer  $(z'_0 - z_0)$ .

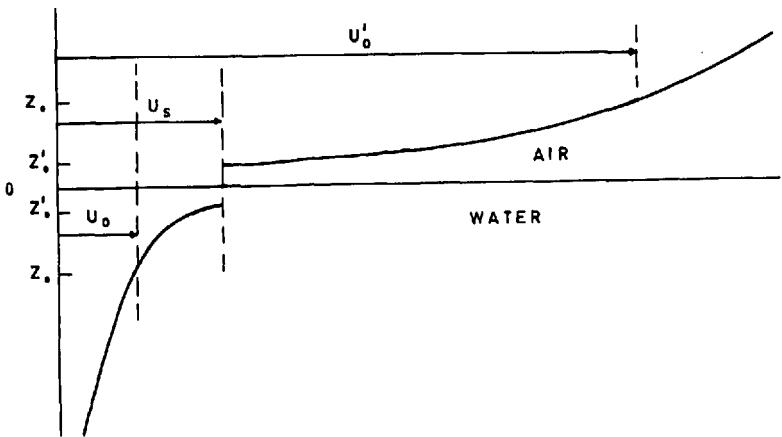


Figure 2. Cartoon of the matching of the air and water velocity profiles.

$$\frac{D_0}{D'_0} = \frac{\tau_s \cdot (\mathbf{u}_s - \mathbf{u}_0)}{\tau_s \cdot (\mathbf{u}'_0 - \mathbf{u}_s)} = \epsilon \quad (43)$$

where  $D_0$  and  $D'_0$  are respectively the dissipation rate/unit area in water and air.

Furthermore, on substituting for  $u_0$  in Eq. (29) from Eq. (36) using Eq. (38), we obtain a relation for  $K_0$  in terms of  $a$  and  $a'$ ,

$$K_0 = \frac{1}{2} \frac{a'}{a^{[2/(1-\epsilon)]}} \quad (44)$$

and also an expression for the ratio ( $\phi$ ) of the reference wind speed ( $u'_0$ ) to the wave speed ( $c_0$ ) of the gravity wave of peak frequency ( $\sigma_0$ ), namely,

$$\phi = \frac{u'_0}{c_0} = \gamma K_0^{1/2} \quad (45)$$

## 6. Observations

The predictions of the similarity hypothesis of Section 5 can be compared with data obtained from profile measurements made in air and water, preferably from experiments in which both profiles were observed simultaneously.

Eq. (38) allows an estimate of  $\gamma$  to be obtained from the roughness relations. On using  $\epsilon = 0.034$ ,  $\kappa = 0.4$ ,  $a = 1.4$  and  $a' = 0.0185$ , we obtain,

$$\gamma \sim 12$$

and using the same parameters, from Eq. (44),

$$K_0 \sim 0.005$$

and from Eq. (45),

$$\phi \sim 0.8.$$

All these estimates are subject to large uncertainties because of the observational variability of  $a'$  and  $\kappa$ , and of the derived quantity,  $a$ . On using the range 0.35 to 0.45 for  $\kappa$ , 1 – 2.5 for  $a$ , and 0.01 – 0.0185 for  $a'$ , we find for example that  $\gamma$  lies in the range 9 – 17. A change in  $a'$  alone from 0.0185 to 0.01 only increases  $\gamma$  from 12 to 13. The uncertainties in the parameters are probably consistent with  $\phi \lesssim 1$  and a physical model in which we regard the air flow as occurring relative to the wave speed of the gravity waves centered in the equilibrium range, through which the momentum is transferred from air to water.

Phillips (1985) has shown that the spectral rate of energy loss from the wave components in the equilibrium range,

$$\epsilon(\mathbf{k}) \sim m\beta(\cos \theta)^{3p} u_*^3 k^{-2}$$

where  $m \geq 0.04$ . This result is based on experimental data on the spectral rate of energy input from the wind, which gives a lower bound for the spectral rate of energy loss at the same wavenumber ( $\mathbf{k}$ ). The spectral rate of energy loss in the coupled layer ( $z_0 - 0 - z_0$ ) centered on the sea surface (Fig. 2), calculated in the same manner, using Eq. (36),

$$\begin{aligned}\epsilon_T(\mathbf{k}) &= \frac{1}{\rho} \overline{\tau_s \cdot (\mathbf{u}'_0(\mathbf{k}) - \mathbf{u}_0(\mathbf{k}))} \\ &\sim \frac{1}{\rho} \overline{\tau_s \cdot \mathbf{u}_0(\mathbf{k})} \epsilon^{-1} \\ &\sim 2\epsilon\beta(\cos\theta)^{3p} u_*^3 k^{-2}\end{aligned}$$

where the overbar denotes an average over the random fluctuations in the shearing stress and drift current fields. The ratio,

$$\frac{\epsilon_T(\mathbf{k})}{\epsilon(\mathbf{k})} \lesssim 2. \quad (46)$$

The inequality (46) is consistent with the dissipation rate in the coupled layer ( $z_0 - 0 - z_0$ ) being due to wave breaking. In a formal sense therefore, the major dissipation flux due to wave breaking is confined to the layer ( $z'_0 - z_0$ ) in air and in water, and the outer regions of the coupled fluids, beyond  $z_0$ , are free to behave essentially as a turbulent boundary layer. The manifestation of this lies in the observed logarithmic profiles. In the water, Toba's constant has a value (Eq. (17)) consistent with this model.

In order to further examine the similarity hypothesis, it is necessary to obtain observations of the water velocity profile. Two quantities ( $u_0$  and  $u_s$ ) must be measured.  $u_0$  can be estimated approximately, without the necessity for observing wave spectra, by measuring the drift velocity at the depth,  $z_0$ , which on expressing  $u_*$  in terms of  $w_*$  in Eq. (23), and substituting  $\epsilon = 0.034$  and  $g = 9.8 \text{ m s}^{-2}$  has the magnitude,

$$z_0 = 125 w_*^2 \text{ m}$$

where  $w_*$  is in  $\text{m s}^{-1}$ .  $u_s$  on the other hand, may only be found from simultaneous measurements of wind and current profiles by logarithmic extrapolation to the intercept ( $u_s, z'_0$ ).

Sets of field data suitable for obtaining  $u_s$  (in which the observed values of  $w_*$  and  $u_*$  were approximately in the theoretical ratio  $(\rho'/\rho)^{1/2}$  for a homogeneous coupled boundary layer) and  $u_0$  have been obtained in Lough Neagh (Bye, 1965), and more recently in the San Diego Model Yacht Pond (Bye, 1987) and other sets of data (Churchill and Csanady, 1983) are available to estimate  $u_0$ .

The mean relations from these data sets for which the individual profile determina-

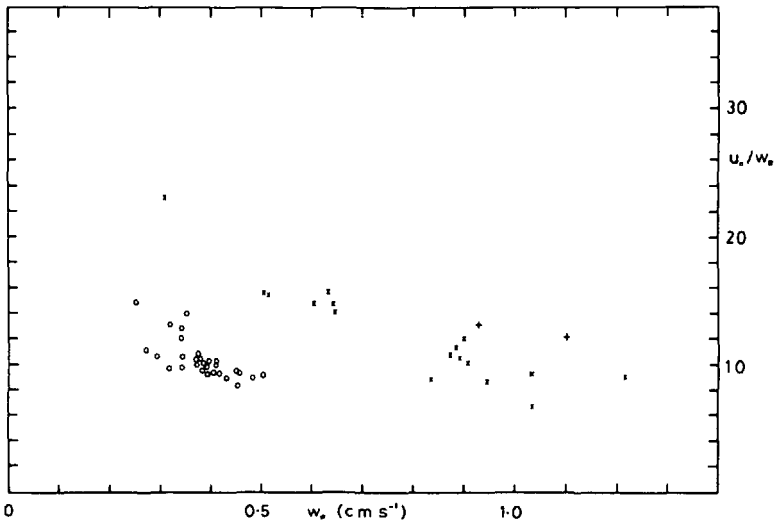


Figure 3. The ratio of the reference velocity for water ( $u_0$ ) to the water friction velocity ( $w_*$ ). + Bye (1965), X Churchill and Csanady (1983),  $\circ$  Bye (1987).

tions are shown in Figures 3 and 4 are  $u_0 = 11 w_*$  and  $u_s = 25 w_*$  which from Eqs. (36) and (39) yield respectively  $\gamma \sim 10$  and  $\gamma \sim 13$ .

These estimates are in good agreement with the value of  $\gamma$  ( $\sim 12$ ) found from the atmospheric data using the similarity theory. We note also that since in the air-sea system  $\epsilon \sim 0.034 \ll 1$  Eqs. (36) and (39) predict that the surface current ( $u_s$ ) defined by the logarithmic profiles, has approximately twice the magnitude of the reference current ( $u_0$ ) defined by the Stokes wave spectrum, and that on applying Eq. (42) at the depth ( $z_1$ ) at which the drift current vanishes,

$$u_s = 0.034 u'.$$

This result is in accord with common observation (e.g. Kraus, 1972).

## 7. Discussion

In the region closer than  $z_0$  to the sea surface it is very difficult to make direct measurements. One approach, on the water side of the interface, is to introduce drifters of depth  $d \leq z_0$ . In the profile runs on the San Diego Model Yacht Pond in which typically  $z_0 \sim 2$  mm, very thin drifters of depths 0.55 mm and 2.5 mm were used, and it was found that their velocities ( $u_F$ ) were very similar, and intermediate between  $u_0$  and  $u_s$ , the mean value (Bye, 1987) was,

$$u_F \sim 16 w_*.$$

This result is identical (probably fortuitously) with  $u_F \sim 16 w_*$  obtained by Wu (1983) from the average of the speeds of surface drifters in wind wave tunnel investigations

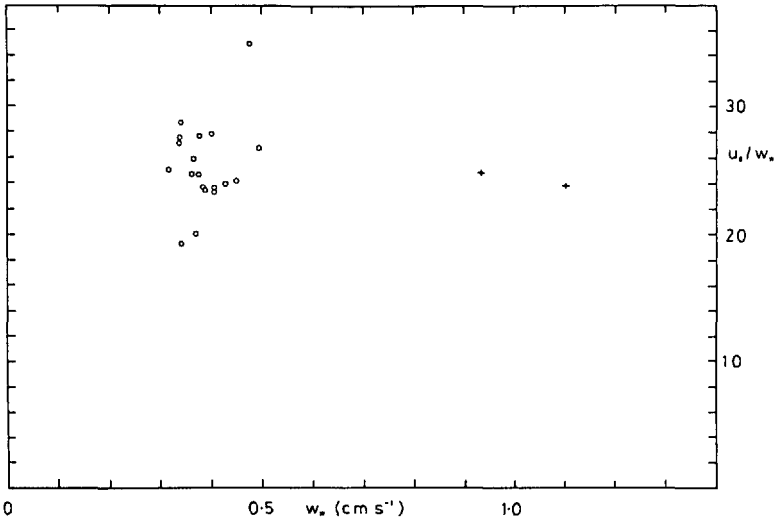


Figure 4. The ratio of the surface current ( $u_s$ ) to the water friction velocity ( $w_*$ ). + Bye (1965), ° Bye (1987).

(The relations for  $u_0$ ,  $u_s$  and  $u_F$  from the San Diego Model Yacht Pond were each estimated to have a standard error of  $\pm 2 w_*$  (Bye, 1987).) We deduce tentatively that  $u_0$  and  $u_s$  are bounds for the observed drift speed of small objects on the sea surface. In reality these objects sample a turbulent shear layer of thickness ( $z_0$ ) during their transit, which occurs in aerodynamically rough flow, vide the prediction of Eq. (24) and Figures 3 and 4.

In summary, it is concluded that:

- (i) The logarithmic profile observed beneath the water surface is consistent with the Stokes drift due to the wave spectrum. In particular, observed values of Toba's constant are consistent with observed values of Von Karman's constant.
- (ii) The fundamental roughness length ( $z_0$ ) for the coupled system may be expressed by a Charnock relation for water in which the constant ( $a$ ) is of order unity. This relation arises from the high wavenumber properties of the wave spectrum, and appears to predict correctly the friction velocities for the generation of waves using the classical transition criteria. The intersection of the velocity profiles at  $z'_0$  determine the surface current ( $u_s$ ).  $z'_0$  lies within the layer in which wave breaking occurs, and the stability of the coupled system presumably determines  $a'$ , and by Eq. (38), also  $\gamma$ . The layer of thickness ( $2z_0$ ) centered on the sea surface would appear to be of decisive importance for the exchange processes and needs much further experimental and theoretical study.

- (iii) Similarity profiles are predicted for the constant shear layers in each fluid such that identical drag coefficients apply at the same distance from the interface.
- (iv) The surface current ( $u_s$ ) and the Stokes reference velocity ( $u_0$ ) are proportional to  $u_*$ , as proposed by Toba (1987). Our analysis also predicts (Eqs. (36) and (39)) that  $u_s$  is approximately twice  $u_0$ .

*Acknowledgments.* Helpful comments by the referees are gratefully acknowledged.

#### REFERENCES

- Bye, J. A. T. 1965. Wind-driven circulation in unstratified lakes. *Limnol. Oceanogr.*, 10, 451–458.
- 1967. The wave drift current. *J. Mar. Res.*, 25, 85–102.
- 1985. Large-scale momentum exchange in the coupled atmosphere-ocean, in *Coupled Ocean—Atmosphere Models*, J. C. J. Nihoul, ed., Elsevier Amsterdam, 56–61.
- 1987. Observations of drift velocity, wind and temperature profiles on the San Diego Model Yacht Pond (1965–1967). *Cruise Rep. 12*, Flinders Institute for Atmospheric and Marine Sciences, The Flinders University of South Australia.
- Chang, M-S. 1969. Mass transport in deep-water long-crested random gravity waves. *J. Geophys. Res.*, 74, 1515–1536.
- Charnock, H. 1955. Wind-stress on a water surface. *Quart. J. Roy. Met. Soc.* 81, 639–640.
- Churchill, J. H. and G. T. Csanady. 1983. Near-surface measurements of quasi-Lagrangian velocities in open water. *J. Phys. Oceanogr.*, 13, 1669–1680.
- Csanady, G. T. 1984. The free surface turbulent shear layer, *J. Phys. Oceanogr.*, 14, 402–411.
- Kahma, K. K. and M. A. Donelan. 1987. A laboratory study of the minimum wind speed for wind wave generation, Res. Rep. Canada Centre for Inland Waters. Burlington, Ontario, Canada. Unpublished manuscript.
- Kenyon, K. E. 1969. Stokes drift for random gravity waves. *J. Geophys. Res.*, 74, 6991–6994.
- Kraus, E. B. 1972. *Atmosphere-ocean Interaction*, Oxford Univ., 284 pp.
- Phillips, O. M. 1985. Spectral and statistical properties of the equilibrium range in wind-generated gravity waves. *J. Fluid Mech.*, 156, 505–531.
- Schlichting, H. 1960. *Boundary Layer Theory*, McGraw-Hill, 647 pp.
- Smith, S. D. 1980. Wind stress and heat flux over the ocean in gale force winds. *J. Phys. Oceanogr.*, 10, 709–726.
- Stokes, G. G. 1847. On the theory of oscillatory waves. *Trans. Camb. Phil. Soc.*, 8, 441–455.
- Toba, Y. 1973. Local balance in the air-sea boundary processes III. On the spectrum of wind waves. *J. Oceanogr. Soc. Japan*, 29, 209–220.
- 1987. Similarity laws of the wind wave and the coupling processes of the air and water turbulent boundary layers. Unpublished manuscript.
- Toba, Y., S. Kawai, and S. J. Joseph. 1985. The TOHOKU wave model in *The SWAMP Group: Ocean Wave Modelling*, Plenum Press, 201–210.
- Wu, J. 1982. Wind-stress coefficients over sea surface from breeze to hurricane. *J. Geophys. Res.*, 87, 9704–9706.
- 1983. Sea-surface drift currents induced by wind and waves. *J. Phys. Oceanogr.*, 13, 1441–1451.